

Supporting Information

Melamine-Assisted Synthesis of Porous V₂O₃/N-doped Carbon Hollow Nanospheres for Efficient Sodium-Ion Storage

*Jiaxin Yao^a, Heng Zhang^b, Zejun Zhao^c, Zhixiao Zhu^c, Jialing Yao^a, Xiaoyan Zheng^{*a}, Yong Yang^{*c}*

^a Shaanxi Key Laboratory of Degradable Biomedical Materials, Shanxi R&D Center of Biomaterials and Fermentation Engineering, School of Chemical and Engineering, Northwest University, Xian, Shaanxi 710069, China

^b Xi'an Sunward Aeromat Co., Ltd., No.32, Tuanjie South Road, High-tech Development Zone, Xi'an, Shaanxi 710065, PR China

^c State Key Laboratory of Solidification Processing, Center of Advanced Lubrication and Seal Materials, Northwestern Polytechnical University, Xi'an, Shaanxi 710072, P. R. China

*Corresponding author: zy129@126.com, yongyangfj@nwpu.edu.cn

SI

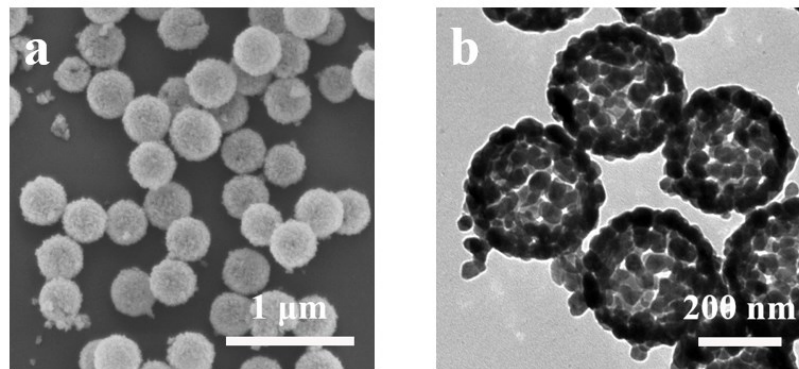


Figure S1. (a) SEM and (b) TEM images of V_2O_3 HSSs.

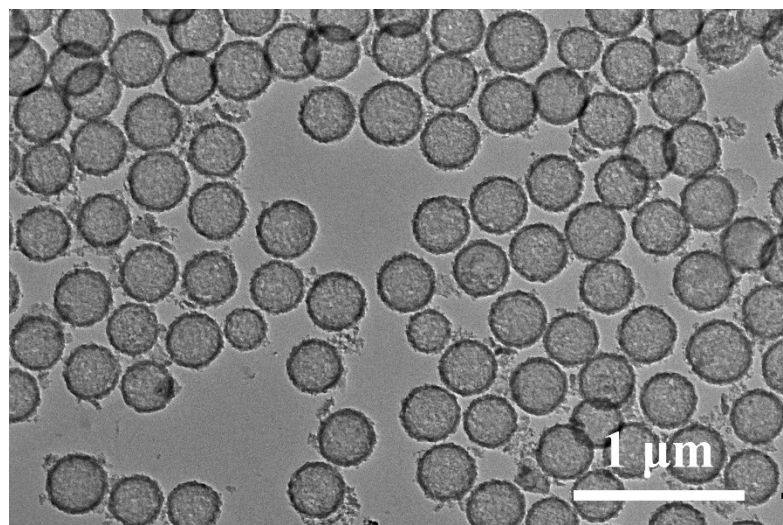


Figure S2. TEM image of the M-VOOH HSs.

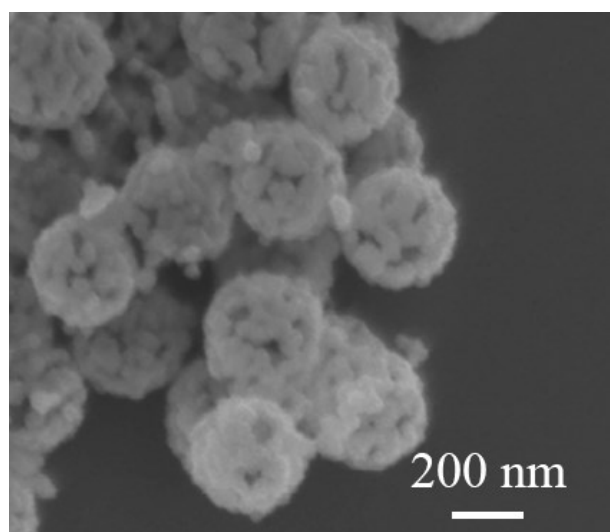


Figure S3. SEM image of the $\text{V}_2\text{O}_3/\text{NC}$ HSs.

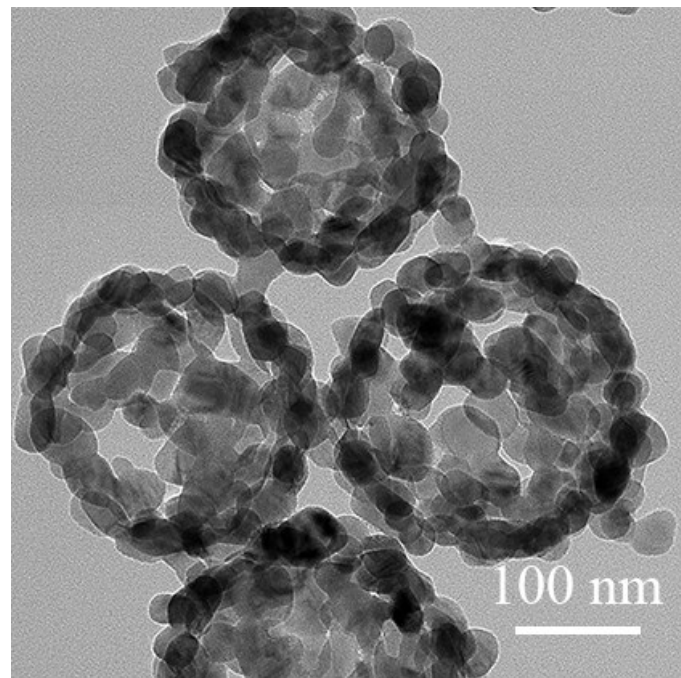


Figure S4. TEM image of the $\text{V}_2\text{O}_3/\text{NC}$ HSs.

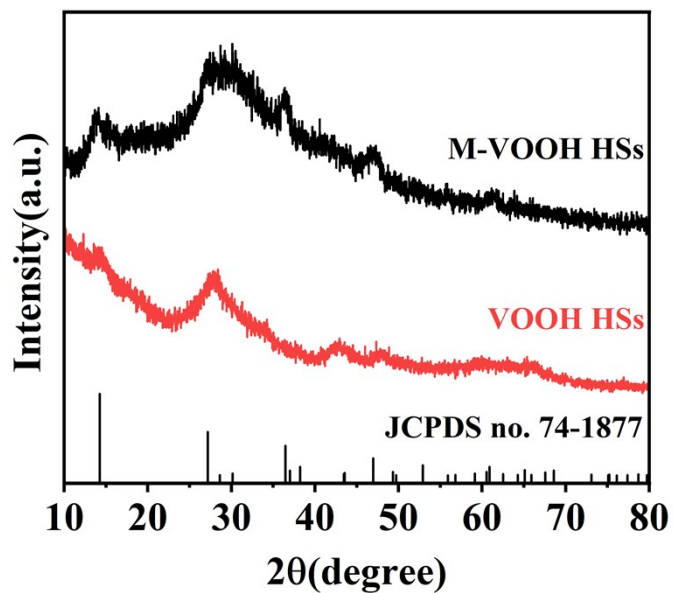


Figure S5. The XRD patterns of M-VOOH HSs and VOOH HSs.

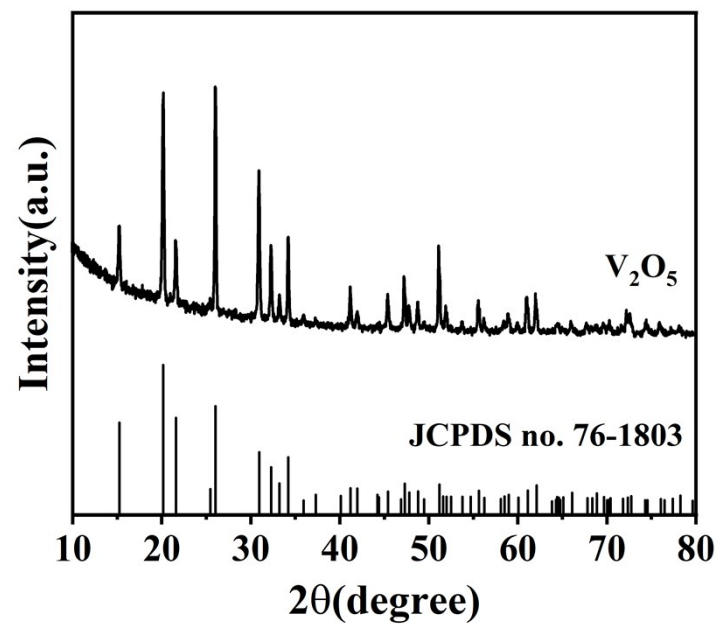


Figure S6. The XRD patterns of the remaining sample after TG test.

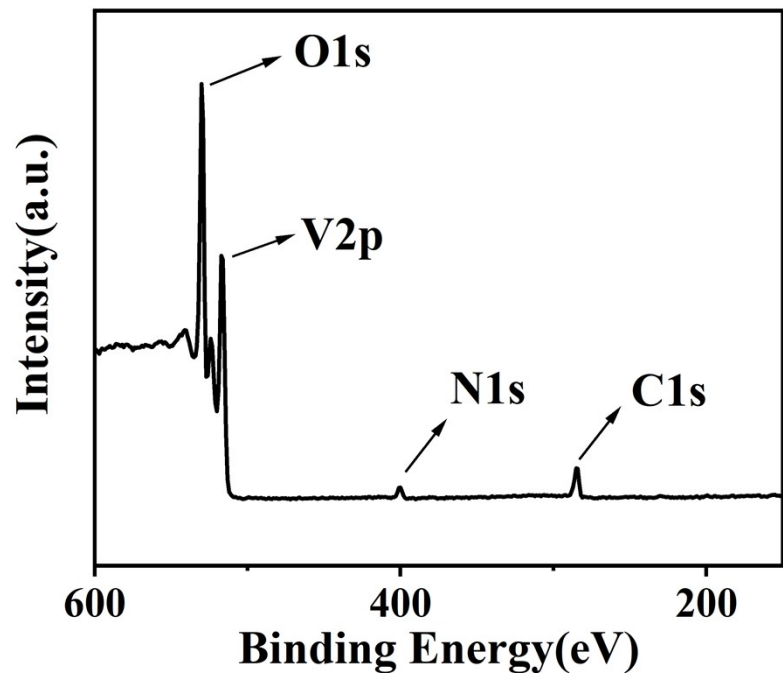


Figure S7. XPS full-spectrum analysis of the $\text{V}_2\text{O}_3/\text{NC}$ HSs.

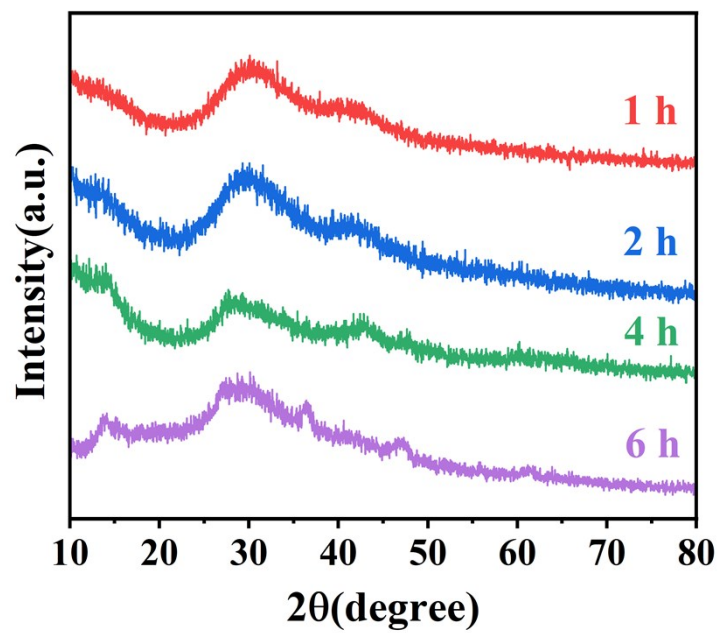


Figure S8. The XRD patterns of the products with hydrothermal reaction time of 1h, 2h, 4h and 6h.

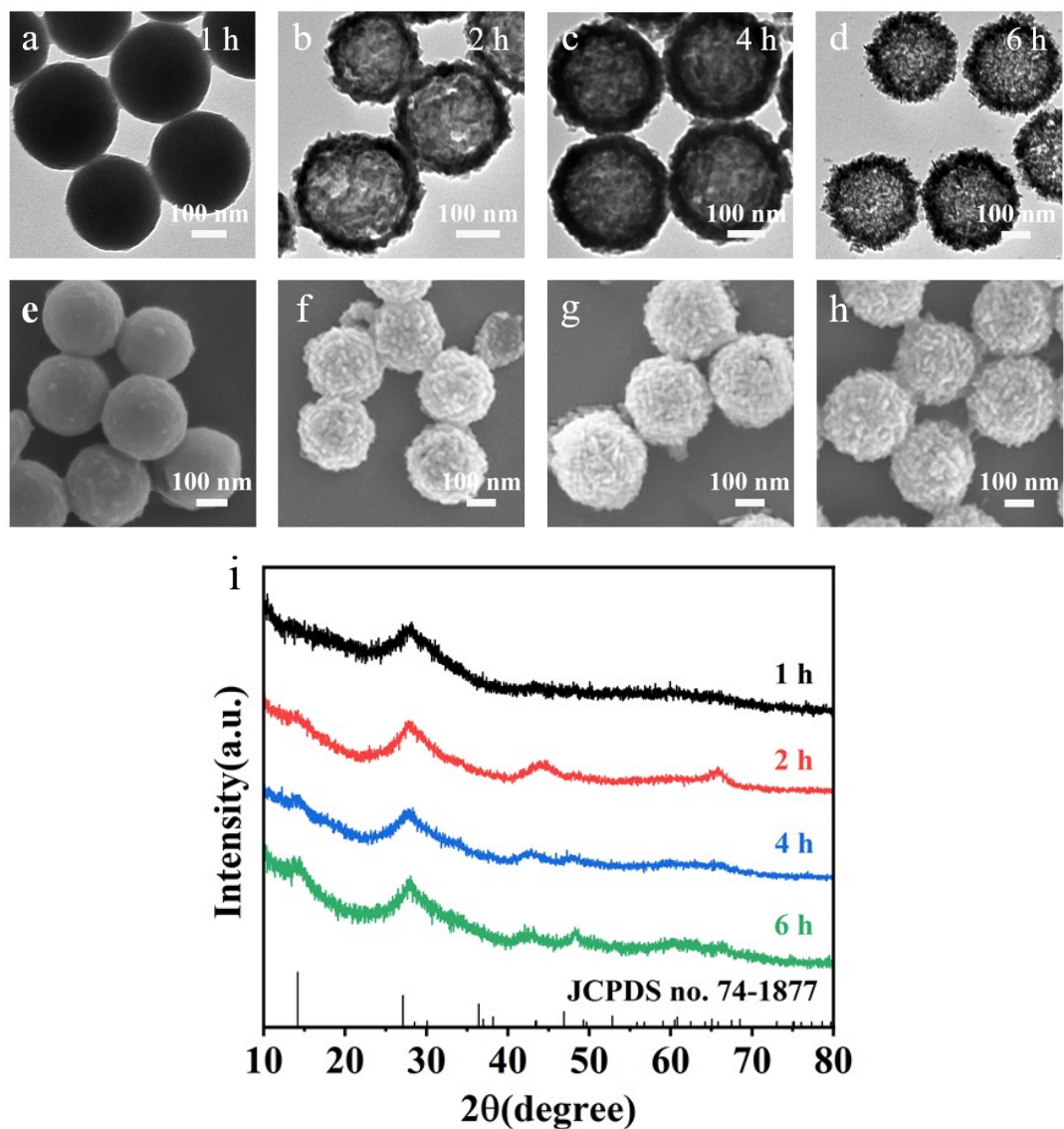


Figure S9. (a-d) TEM, (e-h) SEM images and (i) the corresponding XRD patterns of the products without adding melamine at the hydrothermal reaction time of 1h, 2h, 4h and 6h.

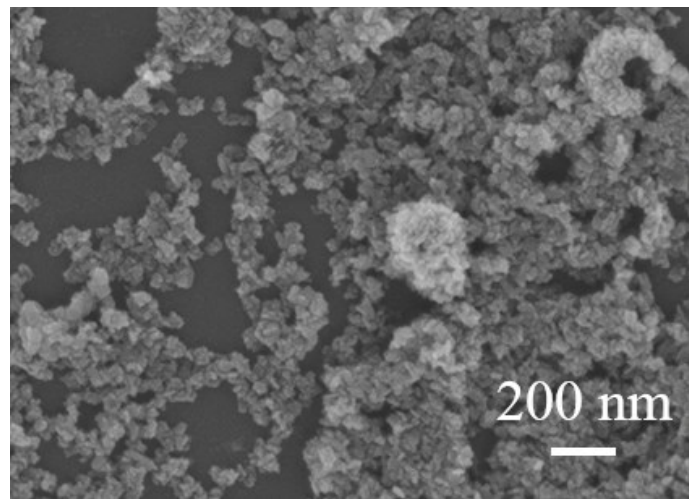


Figure S10. SEM image of hydrothermal reaction products at 160 °C for 4 hours, other conditions were the same as the experimental conditions.

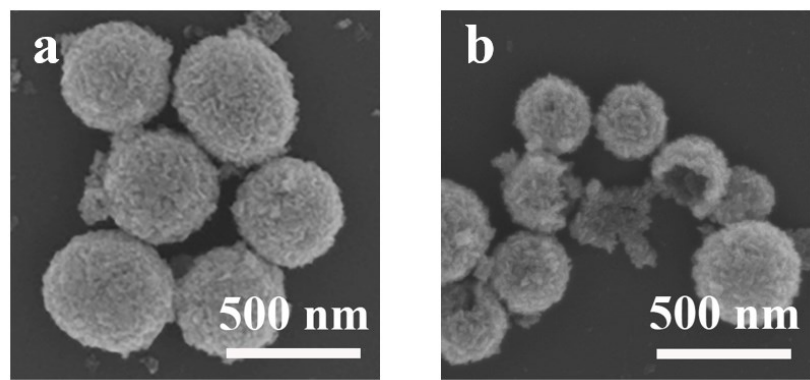


Figure S11. SEM images of the hydrothermal reaction products prepared by adding (a) 40 mg and (b) 60 mg melamine.

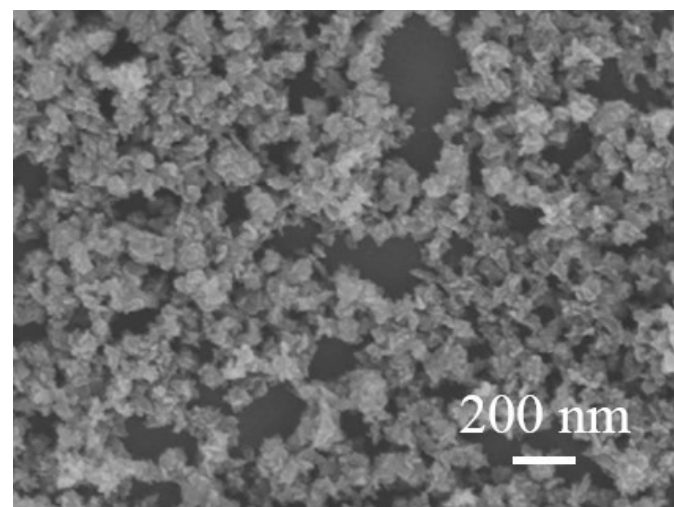


Figure S12. SEM image of the sample synthesized with the help of glucose.

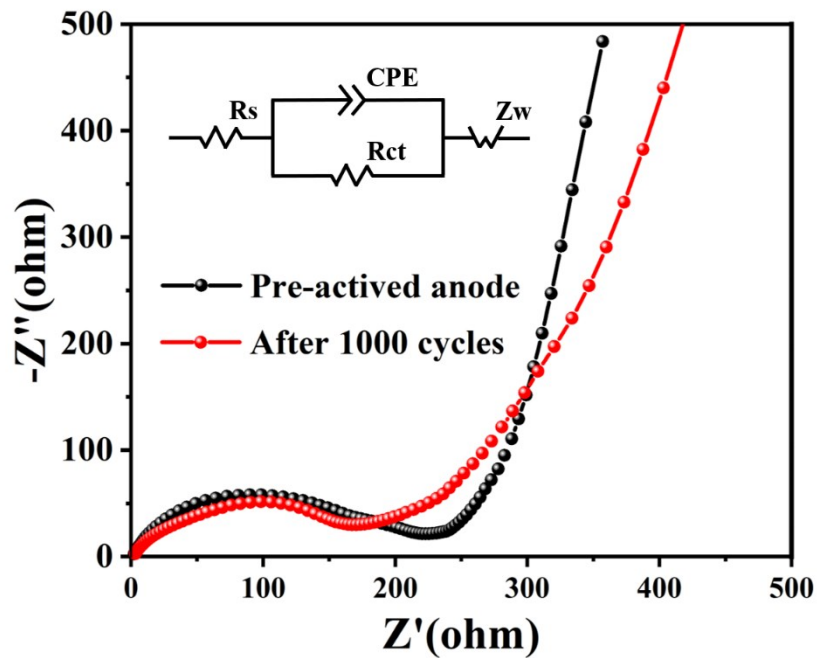


Figure S13. The Nyquist plots of V_2O_3/NC HSs electrode (the illustration shows the equivalent circuit model of the V_2O_3/NC HSs electrode).

The equivalent circuit model of the V_2O_3/NC HSs electrode is composed of series resistance (Rs), constant phase element (CPE), charge transfer resistance (Rct) and Warburg impedance (Zw) element.

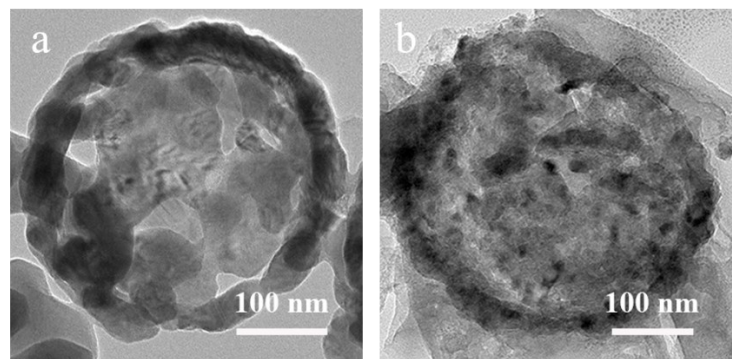


Figure S14. TEM images of $\text{V}_2\text{O}_3/\text{NC}$ HSs (a) before 1000 cycles, (b) after 1000 cycles.

It can be seen that $\text{V}_2\text{O}_3/\text{NC}$ HSs still maintain their original hollow sphere structure after 1000 cycles. It was further confirmed that $\text{V}_2\text{O}_3/\text{NC}$ HSs showed excellent mechanical properties and could resist large volume changes caused by sodium insertion/extraction during the cycle.

Table S1. In this work and previous research, the performance of batteries using V_2O_3 -based materials as SIBs anodes is compared.

V_2O_3 -based anode materials	Synthesis method	Rate performance (mAh g ⁻¹)	Cycle performance (mAh g ⁻¹)	Reference
$\text{V}_2\text{O}_3/\text{NC HSs}$	hydrothermal method	395.4 (0.05 A g⁻¹) 277 (1 A g⁻¹)	263.8 (1 A g⁻¹, 1000 cycles)	this work
$\text{V}_2\text{O}_3/\text{NG}$ nanobelt	low-temperature hydrothermal method	193 (100 mA g ⁻¹) 130 (1000 mA g ⁻¹)	154 (500 mA g ⁻¹ , 500 cycles)	1
$\text{V}_2\text{O}_3\subset\text{C-NTs}\subset\text{rGO}$	the cetylamine-assisted self-scrolling method electrostatic interaction	165 (20 A g ⁻¹)	175 (5 A g ⁻¹ , 15000 cycles)	2
$\text{V}_2\text{O}_3@\text{rGO}$	hydrothermal protocol			3
$\text{GF+ V}_2\text{O}_3/\text{CNTs}$	solvothermal method chemical vapor deposition	612 (0.1 A g ⁻¹) 462 (10 A g ⁻¹)	402(2 A g ⁻¹ , 6000 cycles) 134(10 A g ⁻¹ , 10000 cycles)	4
$\text{GF+ V}_2\text{O}_3$	solvothermal method chemical vapor deposition	411 (0.1 A g ⁻¹) 23 (10 A g ⁻¹)	115(2 A g ⁻¹ , 6000 cycles)	4
$\text{V}_2\text{O}_3/\text{C}$ composite	sequential self-template mechanism	216 (100 mA g ⁻¹) 176 (1000 mA g ⁻¹)	173 (1000 mA g ⁻¹ , 2000cycles)	5
V_2O_3 porous nanotubes	reduction process	284 (100 mA g ⁻¹) 167 (1000 mA g ⁻¹)	90 (2000 mA g ⁻¹ , 5300cycles)	6
porous $\text{V}_2\text{O}_3/\text{carbon}$ nanocomposite	hydrothermal approach	270.8 (100 mA g ⁻¹)	145 (1000 mA g ⁻¹ , 1000 cycles)	7
porous shuttle-like $\text{V}_2\text{O}_3/\text{C}$	self-template approach	242 (100 mA g ⁻¹)	133 (2000 mA g ⁻¹ , 1000 cycles)	8

REFERENCES

- [1] J. Zhang, Q. Li, Z. Liao, L. Wang, J. Xu, X. Ren, B. Gao, P. K. Chu and K. Huo, *ChemElectroChem*, 2018, **5**, 1387-1393.
- [2] S. Tan, Y. Jiang, Q. Wei, Q. Huang, Y. Dai, F. Xiong, Q. Li, Q. An, X. Xu, Z. Zhu, X. Bai and L. Mai, *Adv. Mater.*, 2018, **30**, 170712.
- [3] X. Liu, S. Depaifve, T. Leyssens, S. Hermans and A. Vlad, *Batteries & Supercaps*, 2019, **2**, 1016-1025.
- [4] X. Xia, D. Chao, Y. Zhang, J. Zhan, Y. Zhong, X. Wang, Y. Wang, Z. X. Shen, J. Tu and H. Jin Fan, *Small*, 2016, **12**, 3048-3058.
- [5] Y. Li, S. Zhang, S. Wang, J. Leng, C. Jiang, X. Ren, Z. Zhang, Y. Yang and Z. Tang, *J. Mater. Chem. A*, 2019, **7**, 19234-19240.
- [6] A. Sarkar, A. K. Sinha and S. Mitra, *Electrochim. Acta*, 2019, **299**, 914-925.
- [7] X. An, H. Yang, Y. Wang, Y. Tang, S. Liang, A. Pan and G. Cao, *Sci. China Mater.*, 2017, **60**, 717-727.
- [8] Y. Cai, G. Fang, J. Zhou, S. Liu, Z. Luo, A. Pan, G. Cao and S. Liang, *Nano Res.*, 2018, **11**, 449-463.